Cr^{3+} Binding to DNA Backbone Phosphate and Bases: Slow Ligand Exchange Rates and

Metal Hydrolysis

Wenhu Zhou[1,2], Tianmeng Yu[2], Mahsa Vazin[2], Jinsong Ding[1] and Juewen Liu[1,2,*]

[1]. School of Pharmaceutical Sciences, Central South University, Changsha, Hunan, China, 410013.

[2]. Department of Chemistry, Waterloo Institute for Nanotechnology, University of Waterloo, Waterloo, Ontario, Canada, N2L 3G1.

*Email: liujw@uwaterloo.ca

Fax: (+1) 519-746-0435

Phone: (+1) 519-888-4567 extension 38919

Abstract

The interaction between chromium ions and DNA is of great interest in inorganic chemistry, toxicology, and analytical chemistry. Most previous studies focused on *in situ* reduction of Cr(VI), producing Cr^{3+} for DNA binding. Recently, Cr^{3+} was reported to activate the Ce13d DNAzyme for RNA cleavage. Herein, the Ce13d is used to study two types of Cr^{3+} and DNA interactions. First, Cr^{3+} binds to the DNA phosphate backbone weakly through reversible electrostatic interactions, which is weakened by adding competing inorganic phosphate. On the other hand, Cr^{3+} coordinates with DNA nucleobases forming stable crosslinks that can survive denaturing gel electrophoresis condition. The binding of Cr^{3+} to different nucleobases was further studied in terms of binding kinetic and affinity by exploiting FAM-labeled DNA homopolymers. Once binding takes place, the stable Cr^{3+}/DNA complex cannot be dissociated by EDTA, attributable to the ultra-slow ligand exchange rate of Cr^{3+}. The binding rate follows the order of G > C >T ≈ A. Finally, Cr^{3+} gradually loses its DNA binding ability after storing at neutral or high pH, attributable hydrolysis. This hydrolysis can be reversed by lowering the pH. This work provides a deeper insight into the bioinorganic chemistry of Cr^{3+} coordination with DNA, clarifies some inconsistency in the previous literature, and offers practically useful information for generating reproducible results.

Introduction

Chromium can exist in nine different oxidation states, with Cr^{3+} and Cr(VI) (CrO_4^{2-} or $Cr_2O_7^{2-}$) being the most stable forms. While Cr^{3+} is considered as a nutritional supplement,[1] Cr(VI) is highly carcinogenic.[2] Cr(VI) readily enters cells by anion transport mechanisms, and its toxicity is attributed to DNA damage. However, Cr(VI) alone does not damage DNA under physiological buffer conditions without a reducing agent. In one case, microsomes and NADPH were added to mimic the reducing condition *in vivo*; otherwise little DNA binding was detected.[3] *In vivo*, Cr(VI) can be reduced by biological reducing agents.[4, 5] For example, reduction of Cr(VI) by ascorbate resulted in DNA binding and cleavage.[6] Guanine is the most vulnerable base for oxidative damage by Cr(V).[7] It is generally accepted that the reduction of Cr(VI) to Cr^{3+} is responsible for a wide range of Cr^{3+}-DNA adducts,[8-11] as well as Cr(VI)-related genotoxicity and mutagenicity.[12-15] Since Cr^{3+} is the ultimate reason of DNA damage, the direct interaction between Cr^{3+} and DNA is an important topic. Surprisingly, most previous studies focused on Cr(VI), while Cr^{3+} was much less explored.

Cr^{3+} has a quite unique solution chemistry featured by a very slow ligand exchange rate ($\sim 9 \times 10^{-3}$ h^{-1}) due to its d^3 electronic configuration in an octahedral ligand field, leading to highly kinetically stable complexes.[16] Only a few studies touched on the interaction between Cr^{3+} and nucleosides or DNA. Cr^{3+} can bind to DNA through both phosphate backbone and nucleobases. The interaction between Cr^{3+} and nucleotide phosphate was studied by ^{31}P-NMR.[17] Cr^{3+} binding destabilizes the phosphodiester linkages leading to DNA cleavage under alkaline conditions.[13] Cr^{3+} prefers to bind cytosine and guanine,[18] and guanine binds Cr^{3+} the tightest.[3] However, Salnikow *et al* argued that binding is mainly through the phosphate backbone, and the stronger binding of guanine is due to the formation of G-quartets, which facilitate phosphate interaction.[19]

A quantitative study showed that the N7 position of guanine and its nearest backbone phosphate chelate Cr^{3+} with a binding constant of 3150 M^{-1}.[20] The interaction of Cr^{3+} with double-stranded DNA results in the DNA inter-strand crosslinking.[21] Because of a strong coordination and slow dissociation kinetics, Cr^{3+} can form highly stable Cr^{3+}/DNA lesions,[22] inducing its genotoxicity.[23]

The above literature review indicates some inconsistency on the binding mechanism between Cr^{3+} and DNA. Herein, we systematically studied the binding of Cr^{3+} to both DNA backbone phosphate and nucleobases. Our interest on this topic stems from our recent work on an RNA-cleaving DNAzyme named Ce13d that can use Cr^{3+} as a metal cofactor.[24] DNAzymes are DNA-based catalysts.[25-28] The role of Cr^{3+} in the Ce13d DNAzyme is to bind to the scissile phosphate.[29] Given this mechanism, we studied the phosphate backbone binding *via* DNAzyme cleavage activity, and the nucleobases coordination was characterized through Cr^{3+}-induced DNAzyme inter-strand crosslinking and fluorescence quenching. During our experiment, we noticed the effect of Cr^{3+} hydrolysis. These results provide a solid basis for further studies of the Cr^{3+}/DNA bioinorganic chemistry.

Materials and methods.

Chemicals. The DNA samples were purchased from Eurofins (Huntsville, AL), and their sequences and modifications are showed in Table 1. All of the metal salts were from Sigma-Aldrich and the buffers were from Mandel Scientific (Guelph, ON, Canada). All the solutions were prepared using Milli-Q water.

Table 1. DNA oligonucleotides used in this study. The cleavage site ribo-adenine is denoted by rA, FAM = carboxyfluorescein.

DNA name	Sequence and modifications (from 5′-end)
Ce13d	TTTCGCCATAGGTCAAAGGTGGGTGCGAGTTTTTACTCGTTATAGTGACTCGTGAC
Inactive mutant	TTTCGCCATAGGTCAAAG<u>T</u>TGGGTGCGAGTTTTTACTCGTTATAGTGACTCGTGAC
Sub-FAM	GTCACGAGTCACTATrAGGAAGATGGCGAAA-FAM
FAM-A10	FAM-AAAAAAAAAA
FAM-T10	FAM-TTTTTTTTTT
FAM-C10	FAM-CCCCCCCCCC
FAM-G10	FAM-GGGGGGGGGG

DNAzyme activity assay. In a typical Ce13d activity assay, the enzyme strand (2 μM) and FAM labeled substrate (1 μM) were mixed in buffer (25 mM NaCl, 50 mM buffer with different pH's). The complex was annealed by heating at 95 °C for 3 min followed by slow cooling to room temperature over 30 min. Then, 1 μL metal solution was added to 9 μL DNAzyme to initiate the cleavage reaction. At designated time points, an aliquot of the sample was transferred to 8 M urea containing 1× gel loading dye to quench the reaction. The cleavage product was then separated by a 15% denaturing polyacrylamide gel (dPAGE) and the results were analyzed using a Bio-Rad ChemiDoc MP imaging system.

DNA binding with Cr^{3+}. To study DNA and Cr^{3+} binding, Cr^{3+} (1 mM, 1 μL) and FAM-labeled DNA (10 μM, 1 μL) were mixed in buffer (25 mM NaCl, 50 mM MES, pH 6.5, 9 μL). At each time point, the reaction was stopped by adding 1 μL EDTA (10 mM). Then, the samples were analyzed using the dPAGE as described above.

Cr^{3+} hydrolysis assay. Cr^{3+} (1 mM, 2 μL) was added to buffers (5 mM, 14 μL) of various pH's. After incubation for a designated time, the pH was adjusted by adding MES (2 μL, 500 mM, pH 6.5). Then, 2 μL of the FAM-abeled C10 DNA (10 μM) was immediately added, followed by 2 h incubation. The reaction was stopped by EDTA (10 mM, 2 μL). Afterwards, HEPES buffer (50 mM, 80 μL) was added, and the fluorescence intensity at 525 nm was monitored in a 96-well plate with a microplate reader (M3, SpectraMax) by exciting at 485 nm. To acidify the solution, each 20 μL Cr^{3+} sample was added with HCl (0.1 M, 1 μL) for 1 h incubation.

Results and Discussion

The Ce13d DNAzyme and its mechanism. The secondary structure of the Ce13d DNAzyme is shown in Figure 1A. Its substrate strand contains a single RNA (denoted by rA). The 2′-OH group of this RNA nucleotide acts as an internal nucleophile to attack the scissile phosphate, forming a highly negatively charged phosphorane intermediate. Ce13d is similarly active with all the trivalent lanthanide ions and Y^{3+}, moderately active with Pb^{2+} (~20-fold slower than Ce^{3+}),[29] and weakly active with Cr^{3+} (~150-fold slower than Ce^{3+}).[30] Once the scissile phosphate is replaced by a phosphorothioate linkage, it becomes active with thiophilic metals such as Cd^{2+}, Cu^{2+}, and Hg^{2+}.[29, 31] Therefore, the role of the metals, including Cr^{3+}, is to neutralize the negative charges built in the transition state (Figure 1B). Since Ce13d is the only known DNAzyme that works with Cr^{3+}, it provides a unique opportunity to study the interaction between Cr^{3+} and the DNA phosphate. This information can be obtained by measuring the cleavage activity of the Ce13d DNAzyme.

The H₂O and Cl⁻ exchange does not affect Cr³⁺ activity. Cr^{3+} has a very slow ligand exchange rate due to its d^3 electronic configuration, and this can be explained by the octahedral crystal field stabilization energy theory.[16] A consequence is the extremely slow dissolution of anhydrous salt of $CrCl_3$, due to the slow exchange of Cl^- by water. In this study, we used chromium trichloride hexahydrate as the Cr^{3+} source, which strictly speaking has a formula of $[CrCl_2(H_2O)_4]\cdot Cl(H_2O)_2$.[32] After dissolving this salt, the solution gradually changed its color from green to blue/violet over 3 months due to the formation of $[CrCl(H_2O)_5]\cdot Cl_2(H_2O)$. The time needed for this color change also exemplifies slow exchange (Figure 1C, upper panel). When testing these Cr^{3+} samples with Ce13d, they all induced a similar amount of cleavage (Figure 1C, lower panel). We measured the cleavage kinetics of the freshly prepared and 3-month old Cr^{3+} samples, each yielding a similar cleavage rate of 1.0 h^{-1} (Figure 1D). Therefore, the exchange of Cl^- by water has little effect on the DNAzyme activity, suggesting that both species interact similarly with the DNA phosphate.
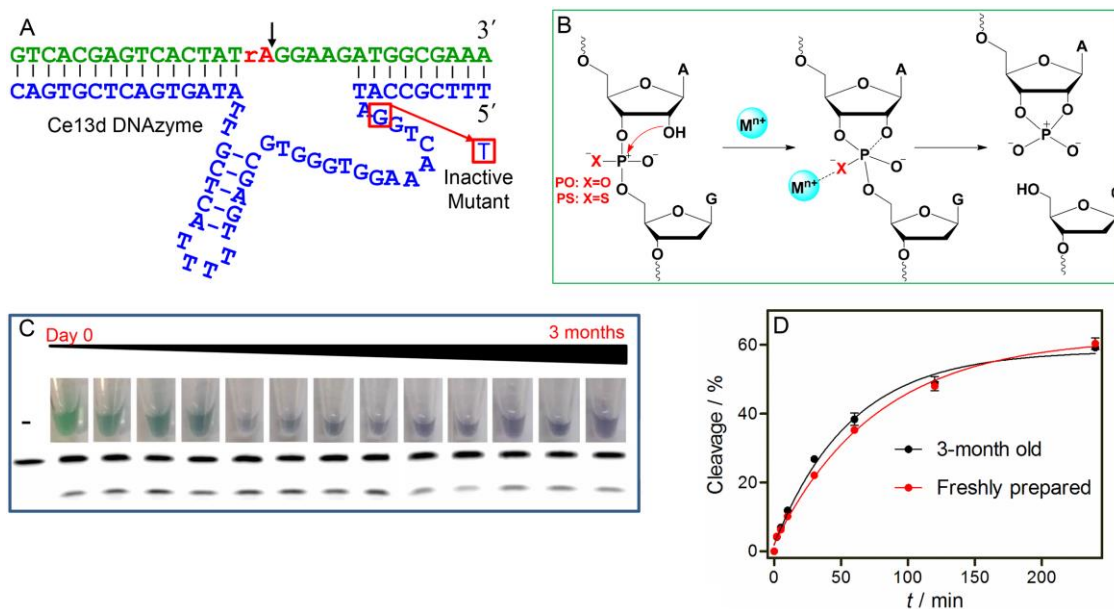
Figure 1. (A) The secondary structure of the Ce13d DNAzyme and an inactive mutant with a single point mutation. The arrowhead indicates the cleavage site in the substrate strand, and rA denotes for ribo-adenine. (B) The general mechanism of RNA cleavage. The 2′-OH acts as an internal nucleophile to attack the scissile phosphate and the role of metal ions is to stabilize the phosphorane transition state. (C) Photographs of the chromium chloride salt dissolved in water from freshly prepared to 3-month old. The bottom panel is the cleavage activity of each tube displayed. They all showed a similar cleavage yield (reaction performed in 25 mM NaCl, 50 mM MES, pH 6.0 for 1 h). (D) Kinetics of substrate cleavage using the freshly prepared and 3-month old Cr^{3+} samples (the final Cr^{3+} concentration was 100 μM).

Effect of pH. pH is an important factor governing DNA/metal interaction. In particular, in the context of RNA cleavage, higher pH is often associated with higher cleavage rates due to facilitated deprotonation of the 2′-OH nucleophile. We measured the cleavage kinetics of the Ce13d at different pH's and their gel images are shown in Figure 2A. This assay was carried out with a FAM-labeled substrate, and we expected to observe two bands in each lane: the uncleaved substrate and the cleavage product. Interestingly, some higher molecular weight bands also appeared, especially between pH 6.0 and 7.0. The origin of these higher bands will be discussed later, and here we first analyzed the pH-dependent cleavage activity.

The relative intensity of the bottom two bands was quantified (Figure 2B), from which the cleavage rate was plotted it as a function of pH (Figure 2C). Interesting, the activity is quite insensitive to pH at slightly acidic conditions (Figure 2C, black dots). The highest rate is at pH 7.0 (~1.3 h^{-1}). However, at this pH, the final yield is only ~40%, which may lead to artifacts in

the rate fitting. Further increasing the pH to 7.6 substantially decreased the cleavage rate. We previously studied the effect of pH using Ce^{3+}, and the cleavage rate increased linearly with a slope of ~0.4 in the pH range of 5.6-6.8 (Figure 2C, yellow dots).[29] The lower pH sensitivity here might be due to hydrolysis of Cr^{3+}, which cancels the general promoting effect of pH for RNA cleavage.
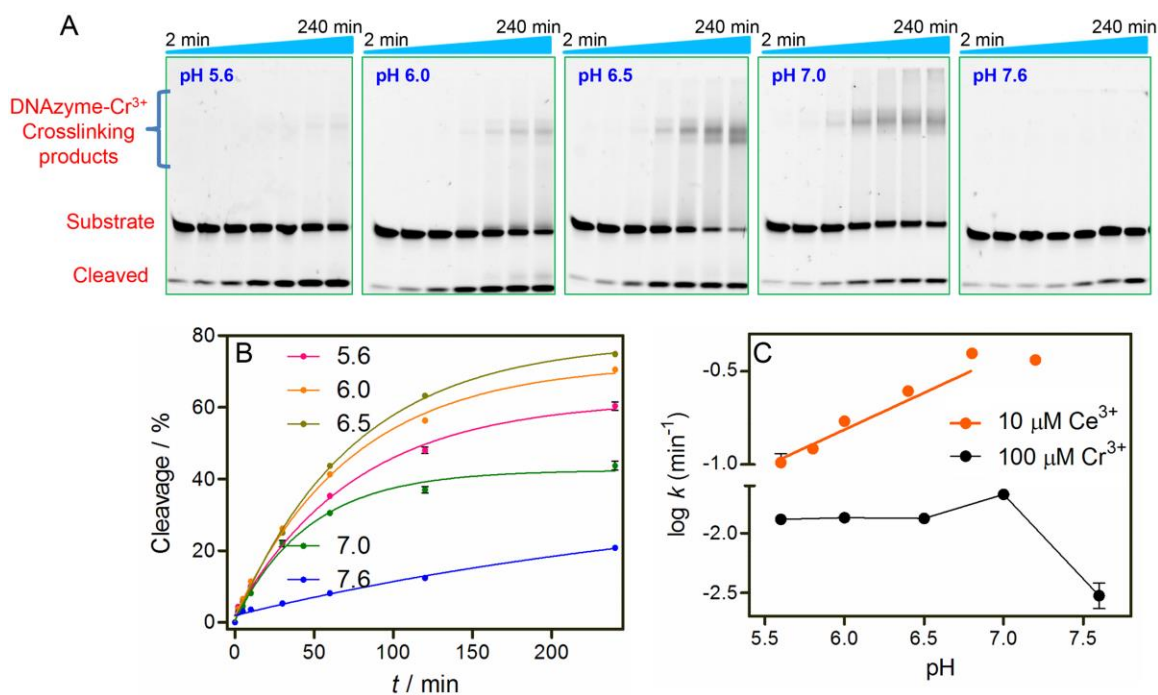

Figure 2. (A) Gel images showing the reaction kinetics of 1 μM Ce13d in the presence of 100 μM Cr^{3+} at different pH's. The assay was carried out in 25 mM NaCl with 50 mM buffer (MES: pH 5.6-7.0; MOPS: pH 7.6). (B) Cleavage kinetics of Ce13d with 100 μM Cr^{3+} at different pH's. (C) The rate-pH profile of Ce13d with 100 μM Cr^{3+} or 10 μM Ce^{3+}.

DNA crosslinked by Cr^{3+}. Next, we shifted our attention to the smeared higher bands in Figure 2A. To identity their origin, we performed the same reaction using the FAM-labeled substrate

alone without the enzyme strand (Figure 3A), where we observed mainly fluorescence quenching with a slightly slower gel running, suggesting those smeared products in Figure 2A must involve also the enzyme strand. Note that the FAM label was only on the substrate, while the enzyme was non-labeled.

Since the Ce13d cleaves the substrate in presence of Cr^{3+} and this complicates our analysis, we next used an inactive Ce13d mutant (Figure 1A). With this single nucleotide mutation, no cleavage was produced with Ce^{3+},[29] and Cr^{3+} should also be inactive. Interestingly, the same smeared higher molecular weight bands were also observed (Figure 3B). Therefore, this feature is independent of the cleavage reaction. The only reasonable explanation is that Cr^{3+} can crosslink double-stranded DNA to form a stable complex. Once formed, it can survive the harsh condition of denaturing gel electrophoresis (e.g. with EDTA and 8 M urea). DNA inter-strand crosslinking by Cr^{3+} was observed under certain *in vitro* conditions.[13, 33] This product is usually used to explain cell cycle arrest by the reduction of Cr(VI), since stable crosslinking products can block the unwinding of duplex DNA and thus DNA replication.[34, 35]

It is also interesting to note that without cleavage, all the substrate strands converted to the crosslinked product in 4 h (Figure 3B). With cleavage (Figure 2A), there is a competition between the crosslinking reaction and the cleavage reaction. We reason that the FAM bearing fragment is released from the enzyme after cleavage,[24] and thus cannot be crosslinked with the enzyme, which is the basis of the competition.

The crosslinking reaction is most pronounced at pH 6.5 and pH 7.0. Even at these optimal pH values, however, the crosslinking kinetics is still relatively slow (requiring 1 h to complete at pH 7). To have a quantitative understanding, we plotted the kinetics of crosslinking (Figure 3C), and further extracted the crosslinking rate as a function of pH (excluding pH 7.6). A faster rate

was observed at higher pH (Figure 4D), which is consistent with a previous study showing that the ligand exchange rate of Cr^{3+} is faster under higher pH.[36] The lack of crosslinking at pH 7.6 may be due to Cr^{3+} hydrolysis (*vide infra*).
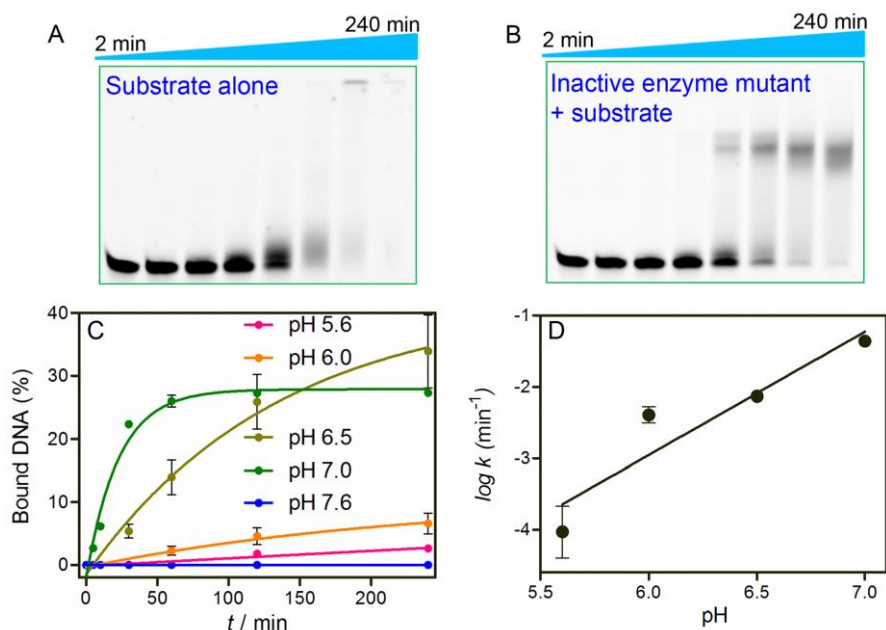

Figure 3. Gel images of Cr^{3+} binding with (A) the substrate alone and (B) the inactive mutated DNAzyme complex. The assay was performed in buffer (25 mM NaCl, 50 mM MES, pH 6.5). (C) Kinetics of crosslinking the Ce13d complex with 100 μM Cr^{3+} at different pH's. (D) The log of DNA crosslinking rate calculated from (C) as a function of pH.

Adding inorganic phosphate to pre-incubated Cr^{3+}/DNAzyme. The inorganic phosphate was previously shown to dissociate Cr^{3+}/DNA binding.[13, 37] On the other hand, we recently used phosphate to mask other metal ions, leaving Cr^{3+} to be the only active metal for the Ce13d DNAzyme.[30] It is also known that Cr^{3+} needs to interact with the scissile phosphate to facilitate the cleavage reaction of the Ce13d.[29] Based on these, we next used free inorganic phosphate to

probe the binding between Cr^{3+} and the DNAzyme. First, the DNAzyme was pre-incubated with Cr^{3+}, and then phosphate was added to test if the pre-formed Cr^{3+}/DNAzyme complex can be dissociated.

To probe phosphate backbone binding (quantified by substrate cleavage), the Ce13d was pre-incubated with Cr^{3+} at pH 5.5 for 1 h (under this pH the crosslinking reaction was minimized). In addition, no Na^+ was included in the buffer to avoid cleavage at this incubation step. Note that Ce13d also requires Na^+ for activity.[38, 39] Then, free phosphate was added together with Na^+, followed by 1 h incubation to induce the cleavage reaction. A low concentration (e.g. <5 mM) of phosphate has little effect on the activity of the DNAzyme, while the cleavage yield started to decrease beyond 5 mM phosphate (Figure 4A, blue trace). The result suggests that Cr^{3+} binds to the DNA phosphate reversibly, and such binding can be dissociated by competition from a high concentration of free phosphate.
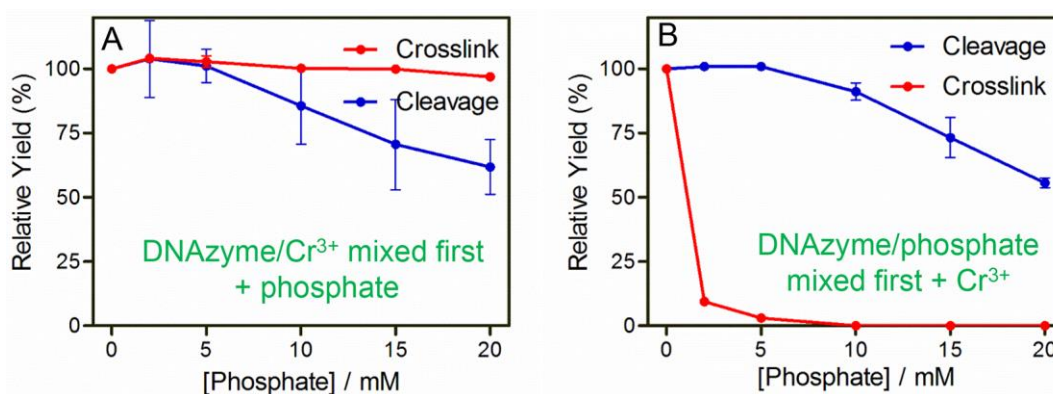

Figure 4. Relatively cleavage and crosslinking yield of the Ce13d in the presence of various concentrations of inorganic phosphate when (A) the DNAzyme and Cr^{3+} were mixed before adding phosphate, and (B) the DNAzyme and phosphate were mixed before adding Cr^{3+}. In (A) 100 μM Cr^{3+} was pre-incubated with 1 μM DNAzyme for 1 h, followed by adding phosphate for 1 h. In (B), 100 μM Cr^{3+} was added to a mixture of phosphate and 1 μM DNAzyme for 1 h. For

the cleavage reaction, the active DNAzyme was annealed in 20 mM Li^+, 50 mM MES, pH 5.5 (pH adjusting by LiOH and HCl). Then, 20 mM Na^+ was added to initiate the cleavage reaction. For the crosslinking reaction, the inactive DNAzyme mutant was annealing in 20 mM Na^+, 50 mM MES, pH 6.5.

To probe the crosslinking reaction, the inactive Ce13d mutant was used and the pH was adjusted to 6.5 to promote crosslinking. In contrast to the cleavage reaction, the crosslinking yield was almost unchanged with phosphate concentration up to 20 mM (Figure 4A, red trace), indicating that the crosslinking products are quite stable (e.g. irreversible binding). Since the crosslinked DNA is not affect by phosphate, we reason that the crosslinking is likely through nucleobases instead of the phosphate backbone of DNA.

Adding Cr^{3+} to the DNAzyme/phosphate mixture. We further switched the order of addition. The DNAzyme was mixed with different concentrations of phosphate first followed by adding Cr^{3+}, directly observing the competition. The cleavage yield has a quite similar trend (Figure 4B, blue trace), further confirming the reversible and quite weak binding to the phosphate. In contrast, the pattern of the crosslinking reaction is totally different. Although phosphate failed to dissociate the crosslinked DNA, it strongly inhibited the crosslinking reaction. With 5 mM phosphate, almost no crosslinking was observed (Figure 4B, red trace). We attribute it to the slow binding kinetic of the crosslink reaction, and Cr^{3+} kinetically prefers to bind with phosphate due to its high concentration (the DNAzyme concentration was only 1 μM).

A few conclusions can be drawn from the above experiments using free phosphate as a probe. Cr^{3+} binds the DNA phosphate reversibly and weakly, while the crosslinking of DNA

bases by Cr^{3+} is strong and irreversible. It is likely that Cr^{3+} binds to phosphate through electrostatic interaction, in which the original coordination sphere of Cr^{3+} remains intact. In addition, we also studied the effect of Na^+ concentration on the cleavage kinetic (Figure S1A). While Ce13d requires Na^+, a decrease of the cleavage rate with higher Na^+ concentration was observed (Figure S1B), likely due to the charge screening effect of Na^+ as a salt. Therefore, for Cr^{3+} binding to DNA phosphate, the affinity is mostly governed by weak electrostatic attraction. On the other hand, the DNA crosslinking reaction is through Cr^{3+} inner sphere binding. In this case, some ligands on Cr^{3+} are displaced by nucleobases, yielding highly stable complexes that cannot be associated by inorganic phosphate.

Effect of DNA sequence. After understanding the interaction between Cr^{3+} and DNA phosphate, we next focused our attention on DNA bases. The data already indicate that Cr^{3+} can stably coordinate with DNA bases, and the products can survive denaturing gel electrophoresis condition. Next, we further studied the effect of different DNA bases using FAM-labeled 10-mer DNA homopolymers. Each DNA (1 µM) was separately incubated with 100 µM Cr^{3+}. Since Cr^{3+} quenches the labeled fluorophore after binding, we used the gel band intensity to quantify Cr^{3+} binding. With a longer incubation time, the band intensity gradually decreased (Figure 5A), and the results are quantified in Figure 5B. Among the four DNAs, the G10 DNA binds to Cr^{3+} the fastest, with a rate of 3.1 h^{-1}. The binding rate of each homo-DNA follows the order of G > C > T ≈ A, although the difference is quite moderate (within 5-fold). In addition, all the DNA sequences reached full Cr^{3+} binding in 4 h. Therefore, each type of nucleobase is capable of coordinating with Cr^{3+} with high stability. This kinetic difference among different DNAs also suggests that Cr^{3+} exerts its quenching function mainly through DNA base binding instead of directly interacting with the FAM fluorophore.

Binding strength/reversibility probed by EDTA. To probe the binding affinity of different DNA bases, we used EDTA as a competitor, which should bind Cr^{3+} much stronger than phosphate does. When 100 µM Cr^{3+} was added to the mixtures of DNA (1 µM) and EDTA (10 mM), no decrease in band intensity was observed for all sequences (Figure 5C, lane 1 and lane 2), suggesting that EDTA inhibited Cr^{3+} binding with DNA. It is likely that EDTA binding is kinetically favored due to its much higher concentration than DNA, just like the above phosphate inhibition experiment.

Next, we tested whether the pre-formed Cr^{3+}/DNA complex can be dissociated by EDTA. For this purpose, 100 µM Cr^{3+} was incubated with 1 µM DNA to form the complex. Then a high concentration of EDTA (10 mM) was added. This time, EDTA failed to recover the DNA fluorescence (Figure 5C, lane 3), suggesting that DNA-Cr^{3+} complex did not dissociate even in the presence of EDTA. Further quantification indicates that EDTA has little effect on the stability of Cr^{3+}/DNA conjugates, suggesting that the complex is highly stable (Figure 5D).

Such strong binding suggests the formation of metallated DNA. We previously tested various metal ions (Cr^{3+} was not included) with DNA, where only Pt^{2+} formed stable metallated DNA adduct.[40] The ligand exchange rate of Cr^{3+} is about 100-fold slower than that of Pt^{2+},[16] and thus Cr^{3+} should have even higher DNA binding stability. Because of such irreversible binding for all the DNA sequences, we cannot quantitatively study the binding strength of each base. Our result confirmed that the binding observed here is through DNA base rather than phosphate backbone, since EDTA can dissociate the phosphate backbone binding.[19]

Binding affinity with different bases. The apparent dissociation constant (K_d) of each DNA homopolymer was measured by respectively incubating them with various concentrations of Cr^{3+} for 4 h. The apparent binding affinity showed a similar trend to that of the binding kinetic, with

15

G > C > T ≈ A (Figure 5E). In a parallel experiment, a longer incubation time of 24 h was carried out, where the relative affinity still followed the same order, but the absolute affinity of each base increased (Figure 5F). This can be explained by the irreversible binding between Cr^{3+} and DNA. Once formed, it cannot dissociate, and thus binding kinetics governed the reaction. In addition, with a longer incubation time, more Cr^{3+} was bound, resulting in higher apparent binding affinity.

After 24 h reaction, the binding of the G10 DNA is saturated at ~20 μM Cr^{3+}, with a K_d of 4 μM Cr^{3+} (Figure 5F). The binding constant between Cr^{3+} and DNA was previously measured to be 3150 M^{-1} or K_d = 310 μM Cr^{3+},[20] which was much weaker than what we measured here. A few factors can give rise to such a difference. First, we used ssDNA, which is more effective for Cr^{3+} binding, while dsDNA was used previously. Second, the reaction time was significantly different (24 h versus 2 h). In addition, we used a higher concentration of Cr^{3+} stock solution and the reaction pH was strictly controlled at 6.5. As it will be discussed later, these two factors also have a strong effect on DNA binding. It needs to be pointed out that even our K_d value is still a conservative estimation. The true binding constant should be extremely high given the irreversible nature of Cr^{3+} binding to DNA. All these measurements (including ours) are kinetically limited, and likely we did not reach the true equilibrium. We did not further extend the incubation time since Cr^{3+} gradually hydrolyzes around pH 6.5 (*vide infra*), which complicates the data analysis.
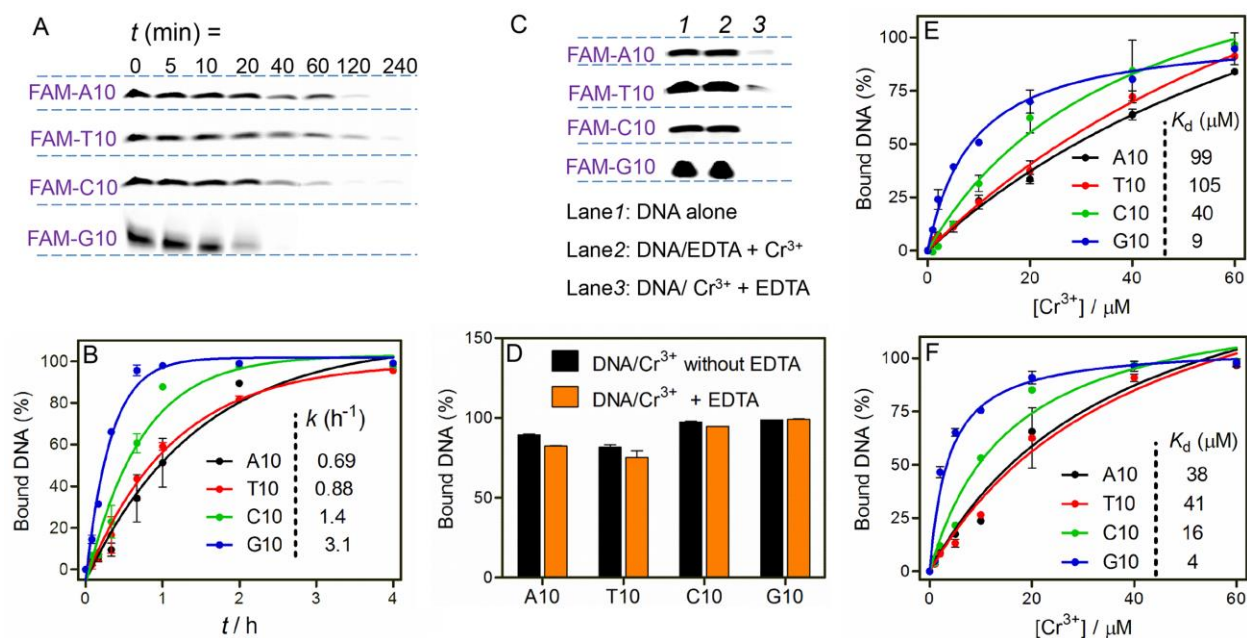
Figure 5. (A) Gel images showing the binding kinetics of 100 μM Cr^{3+} with 1 μM 10-mer DNA homopolymers. (B) Kinetics of Cr^{3+} and DNA binding quantified from (A). (C) Gel images showing DNA mixed with EDTA (10 mM) first and then adding Cr^{3+} (lane 2); and DNA mixed with Cr^{3+} first and then adding EDTA (10 mM, lane 3). (D) Quantification of the last two lanes in (C) normalized to the first lane. The fraction of bound DNA as a function of Cr^{3+} concentration after (E) 4 h and (F) 24 h incubation. All the assay were performed in 25 mM NaCl, 50 mM MES, pH 6.5.

Effect of Cr^{3+} hydrolysis. Metal ions can be hydrolyzed at high pH. Chromium hexahydrate is a strong acid with a pK_a1 of ~4. The above studies showed that at a slight basic pH of 7.6, Cr^{3+} failed to crosslink the DNAzyme, which may be due to hydrolysis. To test this, an experiment was designed as outlined in Figure 6A. Before adding DNA, a few Cr^{3+} solutions were respectively stored in a series of buffers with different pH's. At designated time points, the pH was adjusted to pH 6.5 (the optimal pH for DNA and Cr^{3+} binding), followed by an immediately

addition of 1 μM FAM-C10 DNA. After 2 h incubation, the fluorescence intensity was measured to quantify the fraction of bound DNA.

When stored at pH 3, Cr^{3+} still fully quenched the fluorescence even after storing for 24 h, suggesting quantitative DNA binding (Figure 6B, red trace) and thus the lack of Cr^{3+} hydrolysis at pH 3. Note the pH of a 100 mM Cr^{3+} stock solution is around 3. At pH 5, Cr^{3+} still largely retained the binding ability after 24 h storage, while incubation Cr^{3+} at pH 7 has gradually weakened its DNA binding over time (Figure 6B, yellow trace). The hydrolysis kinetic of Cr^{3+} at pH 9 is even faster, as indicated by the sharp decrease of the bound DNA. The DNA binding kinetics in Figure 6B is a reflection of the hydrolysis of Cr^{3+}. Overall, an elevated pH promotes Cr^{3+} hydrolysis and decreases DNA binding.

Of note, we initially used a dilute Cr^{3+} stock solution (1 mM) to study the DNA binding, and obtained inconsistent results at different days, which is probably due to hydrolysis. The pH of 1 mM Cr^{3+} is ~6, at which Cr^{3+} would gradually hydrolyze, resulting in different DNA binding yields in different days.

We finally explored whether Cr^{3+} can restore its DNA binding ability after hydrolysis. To test this, the hydrolyzed Cr^{3+} sample was acidified using HCl. After 1 h incubation, the sample was further adjusted to pH 6.5, and the FAM-C10 DNA was added. After 2 h, the fluorescence was significant quenched (Figure 6C), suggesting DNA binding and Cr^{3+} hydrolysis is reversible.
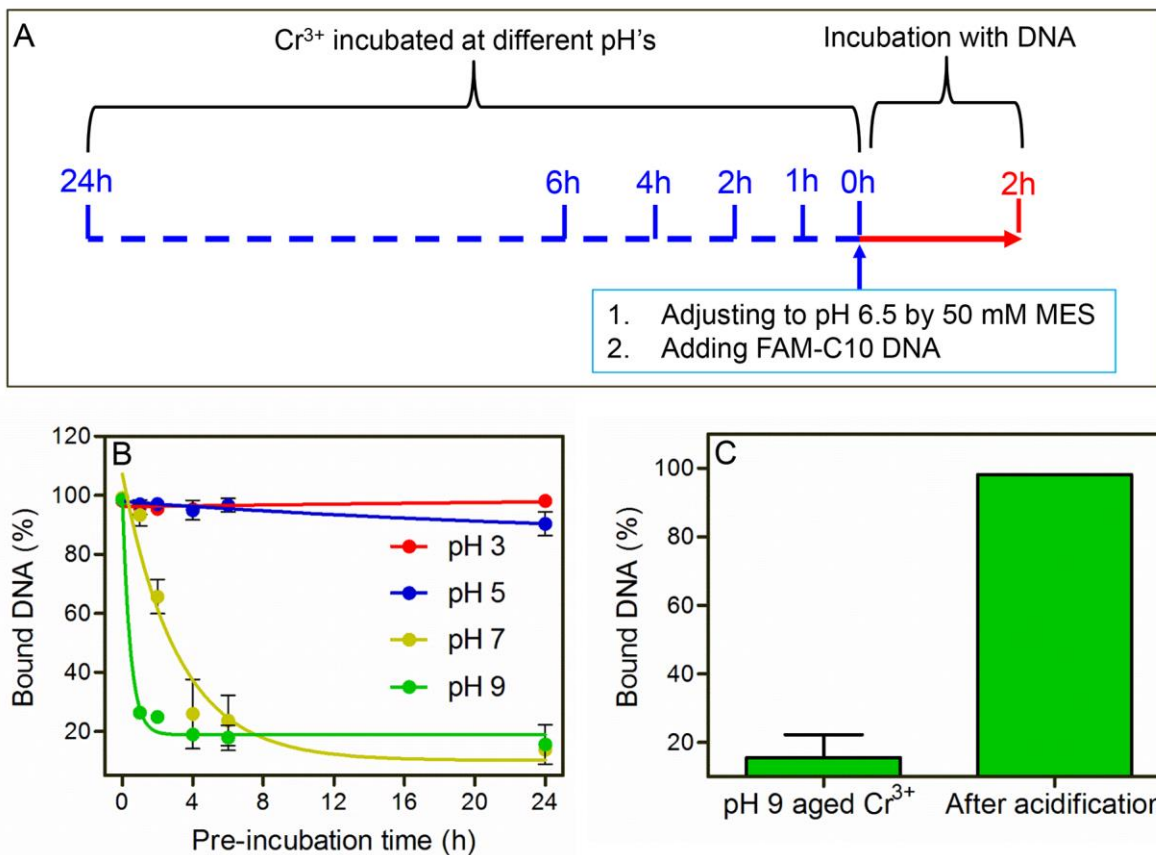
Figure 6. (A) A scheme showing the experiment design to study the effect of Cr^{3+} hydrolysis on DNA binding. (B) Kinetics of Cr^{3+} hydrolysis at different pH's reflected by the quenching of the FAM-C10 DNA. The pH was buffered by acetate (pH 3 and 5), MES (pH 7) and MOPS (pH 9) for Cr^{3+} pre-incubation. (C) The DNA binding ability of hydrolyzed Cr^{3+} sample before and after acidification.

Conclusions

DNA/metal interaction is a highly important topic for drug development, toxicology, materials chemistry, and biosensor development.[41-45] Compared to many other common metals, the work on Cr^{3+} has been quite limited. In this work, we studied the interaction between Cr^{3+} and DNA

by employing the Ce13d DNAzyme and four types of DNA homopolymers. Different from most previously studied metal ions, Cr^{3+} is featured by an extremely slow ligand exchange rate, leading to artifacts for data interpretation. The binding of Cr^{3+} with DNA phosphate was probed by the Ce13d, which is based on the fact that the chemical role of Cr^{3+} in Ce13d catalysis is related to Cr^{3+} binding to the scissile phosphate. Unlike the same reaction catalyzed by Ce^{3+}, where the log of cleavage rate increases with pH with a slope of 0.4, pH has a much smaller effect for Cr^{3+}. This suggests that Cr^{3+} undergoes other reactions that counteract the normal pH effect, likely related to hydrolysis. Using inorganic phosphate as a probe, we demonstrated that Cr^{3+} binding to the DNA backbone phosphate is weak, reversibly, and likely through electrostatic interactions.

The coordination between Cr^{3+} and DNA bases was evidenced by Cr^{3+}-mediated DNAzyme inter-strand crosslinking, forming highly stable products that can survive denaturing gel electrophoresis and even EDTA incubation. The coordination of Cr^{3+} with different bases was further studied using DNA homopolymers. Cr^{3+} quenches the fluorophore labeled on DNA upon binding, which provides a facile way to follow the binding kinetics. Cr^{3+} directly coordinates with all the four DNA bases, forming ultrastable metallated DNA, which cannot be dissociated by EDTA. This is attributable to the slow ligand exchange of Cr^{3+}. The binding kinetic of each base follows the order of G > C > T ≈ A, and this kinetic order also determines the measured apparent K_d. A faster binding and longer reaction time results in a higher apparent binding affinity, where the G10 DNA has the tightest K_d of 4 μM Cr^{3+} after 24 h reaction. The actual K_d is likely to be much lower since the binding is kinetically controlled and true equilibrium was not reached even after 24 h. Cr^{3+} loses its DNA binding ability at higher pH due to hydrolysis, and this process can be reversed by lowering the pH. Taken together, this work

provides comprehensive information about Cr^{3+} and DNA binding, which will enable consistent experimental results for future studies. It has also clarified some inconsistent reports from the previous literature, mainly due to the hydrolysis and slow binding kinetics of Cr^{3+}. The insights from this work can also help understand the toxicity of chromium.

Acknowledgement

References

(1)   Vaidyanathan, V. G.; Asthana, Y.; Nair, B. U. *Dalton Trans* **2013**, *42*, 2337-2346.

(2)   Costa, M.; Klein, C. B. *Crit. Rev. Toxicol.* **2006**, *36*, 155-163.

(3)   Tsapakos, M. J.; Wetterhahn, K. E. *Chem Biol Interact* **1983**, *46*, 265-277.

(4)   Zhitkovich, A. *Chem. Res. Toxicol.* **2005**, *18*, 3-11.

(5)   Levina, A.; Zhang, L.; Lay, P. A. *J. Am. Chem. Soc.* **2010**, *132*, 8720-8731.

(6)   Stearns, D. M.; Kennedy, L. J.; Courtney, K. D.; Giangrande, P. H.; Phieffer, L. S.; Wetterhahn, K. E. *Biochemistry* **1995**, *34*, 910-919.

(7)   Bose, R. N.; Moghaddas, S.; Mazzer, P. A.; Dudones, L. P.; Joudah, L.; Stroup, D. *Nucleic Acids Res.* **1999**, *27*, 2219-2226.

(8)   Salnikow, K.; Zhitkovich, A. *Chem. Res. Toxicol.* **2007**, *21*, 28-44.

(9)   Zhitkovich, A.; Voitkun, V.; Kluz, T.; Costa, M. *Environ. Health Perspect.* **1998**, *106 Suppl 4*, 969-974.

(10)   Xu, J.; Bubley, G. J.; Detrick, B.; Blankenship, L. J.; Patierno, S. R. *Carcinogenesis* **1996**, *17*, 1511-1517.

(11)   Zhitkovich, A.; Voitkun, V.; Costa, M. *Carcinogenesis* **1995**, *16*, 907-913.

(12)   Zhitkovich, A.; Song, Y.; Quievryn, G.; Voitkun, V. *Biochemistry* **2001**, *40*, 549-560.

(13)   Zhitkovich, A.; Shrager, S.; Messer, J. *Chem. Res. Toxicol.* **2000**, *13*, 1114-1124.

(14)   Morse, J. L.; Luczak, M. W.; Zhitkovich, A. *Chem. Res. Toxicol.* **2013**, *26*, 1591-1598.

(15)   Quievryn, G.; Peterson, E.; Messer, J.; Zhitkovich, A. *Biochemistry* **2003**, *42*, 1062-1070.

(16)   Helm, L.; Merbach, A. E. *Chem. Rev.* **2005**, *105*, 1923-1959.

(17)   Wolf, T.; Kasemann, R.; Ottenwälder, H. *Carcinogenesis* **1989**, *10*, 655-659.

(18)   Madhusudanan, K.; Katti, S.; Vijayalakshmi, R.; Nair, B. *J. Mass Spectrom.* **1999**, *34*, 880-884.

(19)   Salnikow, K.; Zhitkovich, A.; Costa, M. *Carcinogenesis* **1992**, *13*, 2341-2346.

(20)   Arakawa, H.; Ahmad, R.; Naoui, M.; Tajmir-Riahi, H.-A. *J. Biol. Chem.* **2000**, *275*, 10150-10153.

(21)   O'Brien, T. J.; Ceryak, S.; Patierno, S. R. *Mutat. Res.* **2003**, *533*, 3-36.

(22)   Levina, A.; Lay, P. A. *Chem. Res. Toxicol.* **2008**, *21*, 563-571.

(23)   Raja, N. S.; Nair, B. U. *Toxicology* **2008**, *251*, 61-65.

(24)   Huang, P.-J. J.; Lin, J.; Cao, J.; Vazin, M.; Liu, J. *Anal. Chem.* **2014**, *86*, 1816-1821.

(25)   Sigel, R. K. O.; Sigel, H. *Acc. Chem. Res.* **2010**, *43*, 974-984.

(26)   Sigel, R. K. O.; Pyle, A. M. *Chem. Rev.* **2007**, *107*, 97-113.

(27)   Ward, W. L.; Plakos, K.; DeRose, V. J. *Chem. Rev.* **2014**, *114*, 4318-4342.

(28)   Lu, Y. *Inorg. Chem.* **2006**, *45*, 9930-9940.

(29)   Vazin, M.; Huang, P.-J. J.; Matuszek, Ż.; Liu, J. *Biochemistry* **2015**, *54*, 6132-6138.

(30)   Zhou, W.; Vazin, M.; Yu, T.; Ding, J.; Liu, J. *Chem. Eur. J.* **2016**, 22, 9835-9840

(31)   Huang, P.-J. J.; Liu, J. *Anal. Chem.* **2014**, *86*, 5999-6005.

(32)   Lennartson, A. *Nat Chem* **2014**, *6*, 942-942.

(33)   O'Brien, T.; Mandel, H. G.; Pritchard, D. E.; Patierno, S. R. *Biochemistry* **2002**, *41*, 12529-12537.

(34)   Snow, E. T. *Environ. Health Perspect.* **1994**, *102 Suppl 3*, 41-44.

(35)   Deans, A. J.; West, S. C. *Nature Reviews Cancer* **2011**, *11*, 467-480.

(36)   Crimp, S. J.; Spiccia, L.; Krouse, H. R.; Swaddle, T. W. *Inorg. Chem.* **1994**, *33*, 465-470.

(37)   Quievryn, G.; Messer, J.; Zhitkovich, A. *Biochemistry* **2002**, *41*, 3156-3167.

(38)   Zhou, W.; Zhang, Y.; Huang, P.-J. J.; Ding, J.; Liu, J. *Nucleic Acids Res.* **2016**, *44*, 354-363.

(39)   Torabi, S.-F.; Lu, Y. *J. Mol. Evol.* **2015**, *81*, 225-234.

(40)   Wang, F.; Liu, J. *Nanoscale* **2014**, *6*, 7079-7084.

(41)   Xiang, Y.; Lu, Y. *Inorg. Chem.* **2014**, *53*, 1925-1942.

(42)   Jamieson, E. R.; Lippard, S. J. *Chem. Rev.* **1999**, *99*, 2467-2498.

(43)   McLaughlin, C. K.; Hamblin, G. D.; Sleiman, H. F. *Chem. Soc. Rev.* **2011**, *40*, 5647-5656.

(44)   Zhang, X. B.; Kong, R. M.; Lu, Y. *Annu. Rev. Anal. Chem.* **2011**, *4*, 105-128.

(45)   Herrera, J. M.; Mendes, F.; Gama, S.; Santos, I.; Navarro Ranninger, C.; Cabrera, S.; Quiroga, A. G. *Inorg. Chem.* **2014**, *53*, 12627-12634.